

Communication

Generalized-Capon Method for Diff-Tomo SAR Analyses of Decorrelating Scatterers

Fabrizio Lombardini ^{1,*} and Francesco Cai ²

¹ Department of Information Engineering, University of Pisa, via Caruso 16, 56122 Pisa, Italy

² formerly with University of Pisa, now at Leonardo S.p.A., via Einstein 35, 50013 Florence, Italy; francesco.cai@leonardocompany.com

* Correspondence: f.lombardini@iet.unipi.it; Tel.: +39-050-2217-511

Received: 27 December 2018; Accepted: 29 January 2019; Published: 18 February 2019



Abstract: In synthetic aperture radar (SAR) remote sensing, Differential Tomography (Diff-Tomo) is developing as a powerful crossing of the mature Differential SAR Interferometry and the emerged 3D SAR Tomography. Diff-Tomo produces advanced 4D (3D+Time) SAR imaging capabilities, extensively applied to urban deformation monitoring. More recently, it has been shown that, through Diff-Tomo, identifying temporal spectra of multiple height-distributed decorrelating scatterers, the important decorrelation-robust forest Tomography functionality is possible. To loosen application constraints of the related main experimented full model-based processing, and develop other functionalities, this work presents an adaptive, just semi-parametric, generalized-Capon Diff-Tomo method, first conceived at University of Pisa in 2013, for joint extraction of height and dynamical information of natural distributed (volumetric) scatterers, with its formalization and a series of insights. Particular reference is given to the important functionality of the separation of different decorrelation mechanisms in forest layers. Representative simulated and P-band forest data sample results are also shown. The new Diff-Tomo method is getting a flexible and rich decorrelation-robust Tomography functionality, and is able to profile height-varying temporal decorrelation, for significantly distributed scatterers.

Keywords: SAR tomography; decorrelation; volumetric scatterers; superresolution image focusing; interferometric information extraction; multidimensional signal processing; array processing; spectral analysis

1. Introduction

In Earth observation by multi-image synthetic aperture radar (SAR) remote sensing [1–4], in particular in coherent SAR data combination [3,4], Differential SAR Tomography (Diff-Tomo) viz. 4D (3D+Time) SAR Imaging [5] is an emerging SAR processing mode (University of Pisa patent). The 4D Diff-Tomo mode can sense and monitor complex dynamic scenes. In fact, in the last decade, Diff-Tomo has been extensively applied to deformation monitoring in urban areas affected by layover effects. It synergically crosses Differential SAR Interferometry for slow motion, i.e., surface deformation monitoring [6], whose core is the temporal phase (rate of change) analysis of repeat-pass acquisition coherent data [6–8], and 3D SAR Tomography [3,4,9–11], getting height resolution by spatial spectral analysis [3,4,9,12] of multi-baseline data. The new mode allows for “opening” the SAR cell resolving in a joint height-deformation velocity domain, the 3rd and 4th dimension, respectively, multiple superimposed scatterers [5]. This is obtained by spatio-temporal spectral estimation, typically of superresolution kind [5,13], of the common largely gapped baseline-time data.

However, Diff-Tomo applications are not limited to urban deformation monitoring [5,13], where the spatio-temporal spectrum to identify is typically discrete, i.e., constituted by two-dimensional lines,

and is related to few layover point-like scatterers with deterministic uniform motions. More recently, with a particular reference to natural scenarios, it has been theorized that possible temporal decorrelation of a scattering component at a given height, corresponding to partially correlated random temporal variations of the complex scattering, produces a continuous distribution of temporal frequencies [14,15]. This is coded by the harmonic Fourier decomposition of a temporal signal, and these temporal frequencies are associated to the spatial frequency related to the height. Such spatio-temporal signatures of temporal decorrelation are originated by phenomena different from the deterministic motions of the urban case, i.e., by physical changes of scatterers over time such as random geometry and dielectric constant changes. Interestingly, these spatio-temporal signatures can be detected by Diff-Tomo processing, up to the identifiability limits [5,14,15]. These are connected to the kind of baseline-time sampling, which can be monostatic or multistatic [10]/pursuit, and to the temporal scale of decorrelation, i.e., short or long-term. This Diff-Tomo detection capability has been shown with real forest P-band SAR data from the BioSAR-1 airborne campaign, subject to mild [15] long-term decorrelation, in which different spatio-temporal signatures of decorrelation of canopy and ground have been identified [1].

Beyond useful phenomenological investigations [1,6], this has led to the development of the concept of 3D Tomography robust to temporal decorrelation phenomena [14,15], which are particularly impacting spaceborne SAR mission planning for forest biomass monitoring [11]. In fact, an advanced temporal decorrelation-robust Tomography can be obtained through higher-order Diff-Tomo processing. Specifically, typical defocusing of coherent 3D tomographic imaging of non fully temporal coherent scenes [3,4,14] can be sensibly mitigated by proper identification in the spatio-temporal frequency domain of the signatures of the temporal decorrelating height-distributed scatterers [15]. The joint consideration of the spatial and the temporal frequency domains can avoid power losses, blurring, and inflated height estimation variance from the misinterpretation of the nuisance temporal harmonic components in the spatial frequency-only 3D focusing [14]. This functionality has been developed in particular with a superresolution model-based generalized-MUSIC Diff-Tomo method [15], as a decorrelation-robust extension of the diffused model-based MUSIC Tomography based on signal subspace fitting. It is important to point out that the MUSIC algorithm, and generalized-MUSIC, are matched to height-compact scatterers; they are approximately matched, and thus also applicable, to volume forest scatterers, if these are not tall. The capability of generalized-MUSIC to reduce temporal decorrelation effects in 3D focusing of such scenarios has also been proven with the P-band forest data [1,16]. This Diff-Tomo method is, however, limited for what concern application scenarios by the adoption of the height-compact scatterers model. In fact, a volumetric scatterer cannot be approximated anymore by the height-compact scatterer model when the volume thickness, in particular the forest canopy thickness, is not negligible w.r.t. the height Rayleigh resolution [3–5]. This situation often stands for forest scenarios of interest and related tomographic campaigns and missions. It is found, especially for, but not limited to, tropical forests, and in particular when the height Rayleigh resolution is fine in large baseline datasets. It is thus important to reduce the application scenario limitations of generalized-MUSIC. Moreover, in addition to this, it can be advantageous to explore and develop other important Diff-Tomo enabled functionalities beyond the already interesting decorrelation-robust Tomography offered by the method.

As a further development in this framework, this work thus presents a contribution that is two fold, algorithmic and functional. Concerning algorithm development, the work extends the Diff-Tomo space-time signature identification of decorrelating height-compact scatterers [1,15] to the important and more general case of decorrelating scatterers that are significantly distributed in height w.r.t. the Rayleigh height resolution. This extension results in a more flexible algorithm than generalized-MUSIC Diff-Tomo, so enlarging the application range. The algorithm, originally conceived at University of Pisa in 2013 (see References [1,16]), is now formalized here and reported together with a series of considerations and insights, and tests extending the original trials. The new reported method, generalized-Capon Diff-Tomo, also constitutes an extension to the space-time domain of the other very

diffused 3D Tomography algorithm, the Capon one, to analyze and handle temporal decorrelating scenarios. Specifically the new method, being of the Capon filters class [5,12], is also able to output scattering power, i.e., reflectivity values, in place of the plain height estimates of the less general model-based subspace fitting methods. Regarding the functional contribution, reference in this work is given in particular, but is not limited, to developing the important functionality of different temporal decorrelation mechanisms separation in forest layers [1]. In fact, advanced stratigraphic analyses of the height-varying temporal coherence of forest scattering, for characterizations in the framework of spaceborne missions development [11], are much more useful than classical ensemble analyses [6]. Interestingly, simulations showed particular potential of the new method for this application, and exploration of additional Diff-Tomo functionalities is thus also extended. Real P-band forest data trials are also reported.

The significance of this two-fold contribution lies in the effort to foster the effective application of the modern Diff-Tomo SAR processing framework to natural environments, and the development of Diff-Tomo based advanced information extraction methods for new SAR remote sensing applications.

After presenting the new generalized-Capon Diff-Tomo for non height compact decorrelating scatterers, main conclusions of the work are that the method appears to be effective and offering promising performance, as indicated by the simulated and real data tests, in particular for separation of temporal decorrelation mechanisms, but also for decorrelation-robust Tomography. This can pave the way to large-scale characterization of vertical structure of temporal decorrelation in forest layers, to application of the decorrelation-robust Tomography processing to tall forest areas, and possibly to the future development of other dynamic information extraction applications in naturally distributed (volumetric) scattering scenarios.

2. Space-Time Generalized Capon Method

The method, semi-parametric adaptive spatio-temporal Diff-Tomo, was first hinted in References [1,16] and is presented with its formalization here. It is super-resolving yet non-parametric in height, to get higher flexibility for volumetric and other distributed scatterers applications, still exploiting the higher-order processing incorporation of a spectral model of the decorrelation in the temporal frequency domain [15]. Reference in this work is to the long-term decorrelation, although the method can be extended, including a short-term decorrelation model [5,14].

Let $\hat{\mathbf{R}}$ be the usual multilook-estimated covariance matrix [4,5,9] of the multi-baseline repeat-pass calibrated data vector, collecting in column-stacked form the corresponding complex pixels for the SAR cell of interest. Additionally, let $\mathbf{a}(f_S, f_T)$ be the space-time steering vector [5,13] determined by the baseline-time acquisition sampling pattern. Parameters f_S, f_T are the generic spatial frequency, coding height, and temporal frequency; they are normalized to the Rayleigh and Fourier frequency resolution [5], respectively. The space-time steering vector codes the form of the data vector component corresponding to a scattering part from a point-like or more generally height-compact scattering component located at (height) f_S , and with temporal frequency f_T , whether from deterministic uniform motion or originated by decorrelation. This data vector component form is a complex two-dimensional space-time harmonic, sampled according to the baselines and acquisition times [5,15]. The starting point of the new Diff-Tomo method is array processing for direction of arrival estimation exploiting a spatial spectrum model [12], a concept that is applied here to the temporal dimension, and extended to the two-dimensional Diff-Tomo processing.

In fact, the spatio-temporal spectrum, i.e., power spectral density (PSD) of a height-extended typically volumetric scattering distribution, affected by temporal decorrelation that can be height-varying [1,15,16], can be considered as the height-continuous superposition of elemental spatio-temporal spectral components that are line shaped in height and continuous in the temporal frequency domain. These elemental spectral components, which are slices of the total spatio-temporal spectrum, are hereafter referred to as ridges, and are shaped in the temporal frequency domain according to the temporal decorrelation behavior. Here, without loss of generality, we will consider

the model for typical long-term decorrelation, with exponential autocorrelation of the complex scattering [6] and thus first order auto-regressive (AR) temporal spectrum [15]. This model was conceived starting from physical considerations of vegetation growth motions and scatterer birth and death processes and validated with real data [6]. It is statistically stationary, simple, and not exhaustive, yet it is very diffused [1,15,16], being well representative, effectively capturing the bulk of decorrelation phenomena, and using a single characterizing parameter. This is the long-term coherence time that is here allowed to be height varying, $\tau_C(f_S)$, and is normalized to the revisit time. The corresponding temporal frequency bandwidth $B_T(f_S)$, two-sided, referred at -3 dB, and normalized to the Fourier resolution, is equal to $(N_{rp}-1)/[\pi\tau_C(f_S)]$, with N_{rp} the number of passes [15], possibly multistatic/pursuit. The temporal frequency bandwidth here constitutes the fourth dimension of the Diff-Tomo estimation problem, beyond the classical third dimension, the tomographic height. A spatio-temporal spectral support and supports of ridge components are exemplified in Figure 1. A possible non-null temporal frequency centroid [15] $\bar{f}_T(f_S)$ can also be included, representing a fifth parameter, capturing long-term average motion or other linear trends of collective phase shift. The temporal frequency shape (temporal PSD) of the generic ridge can thus be coded, after normalization to unit area, as $S_M(f_T; f_S, \bar{f}_T, B_T)$.

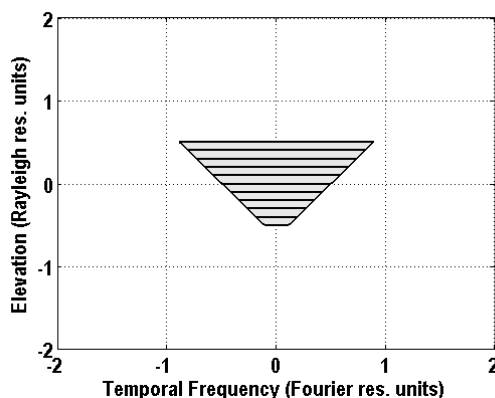


Figure 1. Sketch of spatio-temporal spectrum support and ridge components, decorrelating volume scatterer, -3 dB temporal bandwidth.

To effectively estimate the ensemble of spatio-temporal ridge components, the two-dimensional adaptive Capon estimator [5] has been generalized to be matched to the generic modeled ridge, in place of a plain two-dimensional line component. Like conventional Capon, this generalized-Capon Diff-Tomo filter is designed to minimize the total output power, thus reducing unwanted interference, i.e., spectral leakage, that is especially strong with the typical gapped sampling [5,13], from space-time spectrum portions different from the currently tuned one. However, the tuned component, for which a unit gain constraint is imposed that is now on the statistical power, in place of the deterministic line component amplitude, is the entire spatio-temporal ridge for the height of interest. Resorting to the common quadratic form expression of power at the output of a filter [12], the problem can be formulated as:

$$\min_{\mathbf{w}} \mathbf{w}^H \hat{\mathbf{R}} \mathbf{w} \text{ subject to } \mathbf{w}^H \mathbf{R}_M(f_S, \bar{f}_T, B_T) \mathbf{w} = 1 \tag{1}$$

with \mathbf{w} , depending on f_S, \bar{f}_T, B_T , the filter coefficient vector, H the Hermitian operator, and \mathbf{R}_M the model normalized spatio-temporal covariance matrix component corresponding to the tuned ridge. The first quadratic form expresses the total filter output power to be minimized, the second form codes the power gain that is constrained.

The model normalized covariance matrix in the constraint can be easily defined as:

$$\mathbf{R}_M(f_S, \bar{f}_T, B_T) = \int \mathbf{a}(f_S, \nu_T) S_M(\nu_T; f_S, \bar{f}_T, B_T) \mathbf{a}^H(f_S, \nu_T) d\nu_T \tag{2}$$

when adopting a stationary decorrelation model as done here. In fact, dyad $\mathbf{a}(f_S, \nu_T)\mathbf{a}^H(f_S, \nu_T)$, merely coding in complex, i.e., phasor form the baseline phase shifts corresponding to the height f_S and the temporal phase shifts related to the generic temporal frequency ν_T , is the spatio-temporal covariance matrix corresponding to a generic single space-time harmonic comprehended by the modeled ridge. Since these harmonics, originated by the temporal decorrelation, are mutually uncorrelated, as known for any stationary random process, the various dyads sum up, scaled by the corresponding weight factor constituted by the temporal PSD of the modeled ridge $S_M(\nu_T; f_S, \bar{f}_T, B_T)$. The model normalized spatio-temporal covariance matrix has also explicit closed-form formulation $\mathbf{R}_M(f_S, \bar{f}_T, B_T) = \mathbf{a}(f_S, \bar{f}_T)\mathbf{a}^H(f_S, \bar{f}_T) \odot \mathbf{R}_{TM}(B_T)$. In this formulation, \odot is the Hadamard element-by-element product, and the elements of the temporal-only model matrix \mathbf{R}_{TM} are the samples of the temporal normalized autocorrelation i.e., coherence function, for the height-varying parameter B_T . For the stationary model, these samples are simply taken at the time lags determined by the time acquisition pattern. This explicit formulation codes the fact that the normalized covariance matrix of a temporal decorrelating scattering element, which is the temporal-only matrix \mathbf{R}_{TM} in the case of null height and null temporal frequency centroid, merely includes on \mathbf{R}_{TM} the proper phasor rotations according to the baseline-time pattern, when the height is shifted to f_S and the temporal frequency centroid is shifted to \bar{f}_T . Note that this second formulation of the ridge model covariance matrix, in addition to be computationally useful, is more general than Equation (2), also comprehending the case of a possible non-stationary decorrelation model. However, this possibility is not exploited here. In fact, a simple analytical model of this kind is not yet available, and would lead to too many unknown parameters beyond B_T , and to possible identifiability problems. Nevertheless, the generalized-Capon Diff-Tomo solution that is derived has a general structure validity.

The solution of filtering design (1) is obtained in particular in closed form, by straightforward Lagrange formulation along the lines of [12], leading to the generalized eigenvalue problem of matrix pencil $(\hat{\mathbf{R}}, \mathbf{R}_M(f_S, \bar{f}_T, B_T))$. A 5D Diff-Tomo functional is thus obtained, exploiting the maximum eigenvalue λ_{\max} of $\hat{\mathbf{R}}^{-1}\mathbf{R}_M(f_S, \bar{f}_T, B_T)$, furnishing the output power $P_{GC}(f_S, \bar{f}_T, B_T)$ versus the parameters, that can be of interest or nuisance according to the application. The functional reduces to 4D if the a priori information of null \bar{f}_T [15] can be exploited. Notably, for each height, i.e., f_S of interest, and possibly temporal centroid \bar{f}_T , maximization over the bandwidth allows collecting all the corresponding scattering power, otherwise spread over the temporal frequencies. At the same time, the bandwidth value maximizing the functional furnishes an estimate of the temporal decorrelation level for the height at hand, i.e., of $B_T(f_S)$ or of the corresponding $\tau_C(f_S)$. This results, in addition to the advanced functionality of temporal decorrelation profiling in the height dimension, in achieving the temporal decorrelation-robust Tomography functionality. Generalized-Capon decorrelation-robust Tomography should be more flexible than the previous generalized-MUSIC based one [15], in that it is non-parametric in height; still, being the new method of the adaptive Capon class [5,12], it should have leakage reduction and thus super-resolution capabilities. Interestingly, the method can be considered as an optimized evolution of the empirical temporal frequency integral concept in Reference [14].

3. Sample Simulated and P-Band Data Results

A simulated example of behaviour of the generalized-Capon Diff-Tomo method is reported in Figure 2, showing a realization of output power, in linear scale and normalized to the maximum output, vs. f_S, B_T , with $\bar{f}_T = 0$, from baseline-irregular multi-static data. The simulation regards a baseline-time sampling with three tracks repeated $N_{rp} = 10$ times [15], for a 128 looks cell with a 1 Rayleigh unit thick, i.e., non-compact, volume scatterer, almost height uniform (Gaussian tapering, -0.5 dB at top and bottom heights). SNR is 15 dB, and long-term decorrelation increases, as typically expected, along the height, with minimum $B_T = 0.25(\tau_C = 11.5)$, mild condition) and maximum $B_T = 1.75(\tau_C = 1.6)$, as in Figure 1. Noteworthy, the reported reflectivity information output cannot be produced by generalized-MUSIC, which furnishes height fitting degrees only [15]. Moreover, it can be seen how, finding the temporal bandwidth maximizing the generalized-Capon functional for

increasing heights, i.e., extracting the location of the maximum value in each horizontal line of the picture in Figure 2, an estimate $\hat{B}_T(f_S)$ can be obtained, as marked by the green superimposed plot. The temporal bandwidth estimated profile well resembles the true linearly varying values, although Montecarlo analysis showed some bias, especially at low bandwidths.

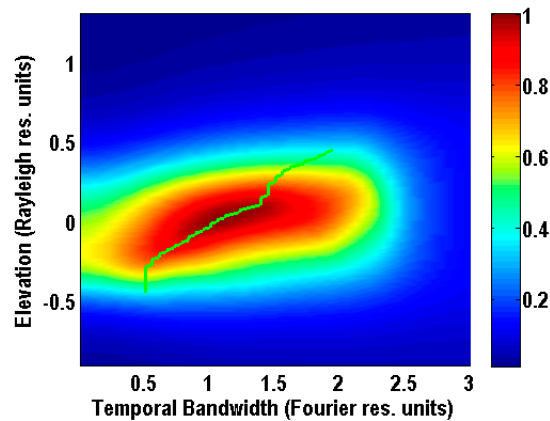


Figure 2. Gen. Capon 4D Diff-Tomo elevation-bandwidth functional, simulated data, output power; green plot shows fit temporal bandwidth.

Additionally, it is interesting that, especially at the higher heights with strong decorrelation, increasing the temporal bandwidth parameter the output power sensibly raises w.r.t. the $B_T = 0$ case at the origin of the bandwidth axis in Figure 2, which, being $\bar{f}_T = 0$ as well, corresponds to plain 3D Capon Tomography [9,15]. This is a sign of the robustness to decorrelation of generalized-Capon based Tomography, also achieved for a non-compact scatterer.

Notably, in addition to the production of the reflectivity information, generalized-Capon is also superior to generalized-MUSIC for a mere height localization of the simulated decorrelating Rayleigh-thick scatterer. In fact, Montecarlo analysis of the estimation accuracy of the height centroid yielded a standard deviation (std) of 0.21 Rayleigh units for the generalized-MUSIC decorrelation-robust Tomography, and a significantly lower std of 0.06 Rayleigh units for the generalized-Capon one.

In Figure 3, sample results are also reported for a multilook cell of the real P-band boreal forest data, HV-pol., from the ESA - DLR Remningstorp airborne campaign BioSAR-1, with mild long-term decorrelation [1,16]. Acquisition baseline-time pattern is quasi-multistatic [15] with $N_{rp} = 3$ passes of three non-simultaneous tracks each, with two month total time span, and processed looks are 17×71 (rg.,az.). The output generalized-Capon power, in arbitrary units, after optimization of the bandwidth parameter for varying f_S, \bar{f}_T is shown in Figure 3a. The two black cross markers on the optimized power peaks in the f_S, \bar{f}_T domain correspond to the ground scatterer and the canopy scattering centroid. The canopy scatterer is weaker than the ground one as typical at P-band [1,11], and the two scatterers are sub-Rayleigh resolved, i.e., super-resolved although not sharply. The slightly non-null and different temporal frequency centroid \bar{f}_T values corresponding to the two scatterers may be due to mere estimation errors, residual miscalibration, or trends of phase shifts from physical phenomena that are not explored here.

Figure 3b reports the optimized parameter $\hat{B}_T(f_S, \bar{f}_T)$ that produced the previous output. Reading the fit temporal bandwidth, now color-coded and expressed in *cycles/months*, at the detected power peaks (see the reported markers), a low estimate \hat{B}_T is obtained for the ground, and a larger \hat{B}_T for the canopy. This is in agreement with the canopy scatterer being the expected more quickly decorrelating one. Far from power peaks, where no significant scattering contribution is present, fitting locks to thermal noise. Application of the method to three land hectares of BioSAR-1 data yielded average $\hat{\tau}_C = 6$ and 13 months for canopy and ground, respectively. These results are consistent with and complement values from dedicated ground-based radar-array tower ESA experiments.

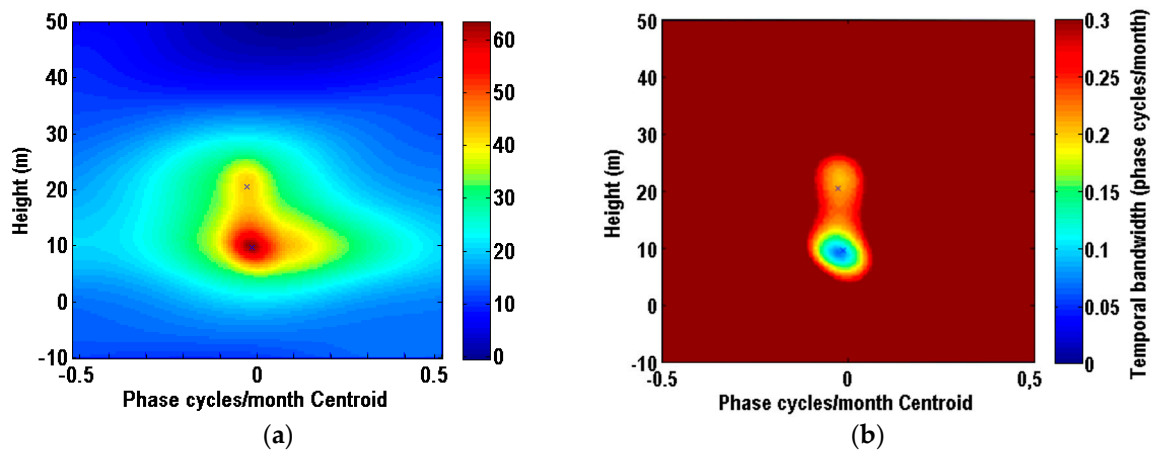


Figure 3. Gen. Capon 5D Diff-Tomo elevation-temporal frequency centroid functional, P-band forested cell: (a) robust output power; and (b) fit temporal bandwidth.

The experimental indications that can be drawn from these simulated and real data tests are that the semi-parametric adaptive generalized-Capon Diff-Tomo method is able both to profile height-varying temporal decorrelation, and to also get the decorrelation-robust Tomography functionality for height-distributed non-compact scatterers, with super-resolution and outputting power distributions along height, as targeted.

4. Discussion and Conclusions

The reported results illustrated and proved the concept of semi-parametric adaptive Diff-Tomo processing by a space-time generalized-Capon algorithm. It was shown that it is possible to jointly estimate heights, temporal bandwidths, and possibly temporal frequency centroids, of interest (or nuisance yet important) in various natural scenarios with distributed scatterers and temporal decorrelation, without resorting to a particular height distribution model. This overcomes possible application constraints of the fully model-based generalized-MUSIC Diff-Tomo in Reference [15], matched to compact scatterers. Moreover, again significantly improving over the previous method [15], the presented generalized-Capon Diff-Tomo, in addition to be more flexible as exemplified by the height accuracy simulated comparison, outputs power values viz. reflectivity estimates. The capability of producing quantitative scattering distributions, in particular in the height domain, in place of plain height estimates not associated to reflectivity values, further enlarges the application possibilities. In fact, generalized-Capon also constitutes a temporal decorrelation-robustified version of plain 3D Capon, as noted from the simulated output power comparison.

On the other hand, for specific applications like mere height localization, robust in presence of temporal decorrelation, in the particular non-frequent condition of compact scatterers, the fully model-based processing [15] may be more accurate. Lower variance of the height estimates can be achieved according to scatterer thinness exploiting the correctly or reasonably matched height model, i.e., exploiting a-priori information. Nevertheless, semi-parametric adaptive generalized-Capon Diff-Tomo appears to be globally more promising. It opens the possibility of applying Diff-Tomo remote sensing to a wider range of natural distributed typically volumetric scattering scenarios. Additionally, it can allow developing new remote sensing applications, based on functionalities going beyond the already advanced decorrelation-robust Tomography in References [15,16], exploiting the peculiar estimates of temporal bandwidths and possibly temporal frequency centroids. In sum, the presented method appears to be more flexible, can be generally better performing, and produces richer output than the first Diff-Tomo based robust Tomography concept originated for particular forest scenes in [15,16], for more general tall forests or different applications, in other scenarios or related to dynamic information extraction.

In conclusion, accounting for the current sample simulated and the real data results, generalized-Capon Diff-Tomo appears to exhibit particularly promising performance for the functionality of decorrelation profiling in forest layers; first-cut more extended simulated analyses including a monostatic case and additional presence of short-term decorrelation are also positive in this direction. The P-band real airborne boreal forest data tests also indicate possible applications for a decorrelation-robust Tomography more general than that in References [15,16], in terms particularly of the retrieved information, i.e., reflectivity distribution in addition to height localization, yet also of the handleable canopy thickness, or for other Diff-Tomo dynamic information extraction functionalities, especially for natural scenarios. Future research is in order, in particular on extensive simulated characterizations of the generalized-Capon Diff-Tomo method, including further height localization accuracy comparisons with generalized-MUSIC, and on developing the large-scale application of generalized-Capon for phenomenological analyses of vertical structure of forest temporal decorrelation. Extension of its application for decorrelation-robust Tomography with reflectivity output will also be considered, together with an investigation of possible trends of phase shift, and method tuning and application to other types of forests and scenes.

Author Contributions: Conceptualization, F.L.; Methodology, Software, Validation, Formal Analysis, Investigation, F.C. and F.L.; Resources, Data Curation, Writing-Original Draft, F.L.; Writing-Review & Editing, F.C. and F.L.; Visualization, F.C.; Supervision, F.L.

Funding: This research received no external funding.

Acknowledgments: The Authors would like to thank the anonymous Reviewers for their comments that helped improving the manuscript presentation.

Conflicts of Interest: The authors declare no conflict of interest.

References

1. Lombardini, F.; Viviani, F.; Cai, F.; Dini, F. Forest temporal decorrelation: 3D analyses and processing in the Diff-Tomo framework. In Proceedings of the IEEE IGARSS, Melbourne, Australia, 21–26 July 2013; pp. 1202–1205.
2. Bruzzone, L.; Marconcini, M.; Wegmuller, U.; Wiesmann, A. An advanced system for the automatic classification of multitemporal SAR images. *IEEE Trans. Geosci. Remote Sens.* **2004**, *42*, 1321–1334. [[CrossRef](#)]
3. Reigber, A.; Moreira, A. First demonstration of airborne SAR tomography using multibaseline L-band data. *IEEE Trans. Geosci. Remote Sens.* **2000**, *38*, 2142–2152. [[CrossRef](#)]
4. Pardini, M.; Papathanassiou, K. On the estimation of ground and volume polarimetric covariances in forest scenarios with SAR tomography. *IEEE Geosci. Remote Sens. Lett.* **2017**, *14*, 1860–1864. [[CrossRef](#)]
5. Lombardini, F. Differential tomography: A new framework for SAR interferometry. *IEEE Trans. Geosci. Remote Sens.* **2005**, *43*, 37–44. [[CrossRef](#)]
6. Rocca, F. Modeling interferogram stacks. *IEEE Trans. Geosci. Remote Sens.* **2007**, *45*, 3289–3299. [[CrossRef](#)]
7. Aiazzi, B.; Alparone, L.; Baronti, S.; Garzelli, A. Coherence estimation from multilook incoherent SAR imagery. *IEEE Trans. Geosci. Remote Sens.* **2003**, *41*, 2531–2539. [[CrossRef](#)]
8. Balz, T. InSAR processing for advanced SAR mode data. In Proceedings of the IEEE PIERS, Shanghai, China, 8–11 August 2016; pp. 5116–5120.
9. Huang, Y.; Ferro-Famil, L.; Reigber, A. Under-foliage object imaging using SAR tomography and polarimetric spectral estimators. *IEEE Trans. Geosci. Remote Sens.* **2012**, *50*, 2213–2225. [[CrossRef](#)]
10. Azcueta, M.; Tebaldini, S. Non-cooperative bistatic SAR clock drift compensation for tomographic acquisitions. *Remote Sens.* **2017**, *9*, 1087. [[CrossRef](#)]
11. Scipal, K. The Biomass mission—ESA’S P-band polarimetric, interferometric SAR mission. In Proceedings of the IEEE IGARSS, Fort Worth, TX, USA, 23–28 July 2017; pp. 3836–3837.
12. Hassaniien, A.; Shahbazpanahi, S.; Gershman, A.B. A generalized Capon estimator for localization of multiple spread sources. *IEEE Trans. Signal Process.* **2004**, *52*, 280–283. [[CrossRef](#)]
13. Reale, D.; Fornaro, G.; Pauciuillo, A.; Zhu, X.; Bamler, R. Tomographic imaging and monitoring of buildings with very high resolution SAR data. *IEEE Geosci. Remote Sens. Lett.* **2011**, *8*, 661–665. [[CrossRef](#)]

14. Lombardini, F.; Cai, F. 3D tomographic and differential tomographic response to partially coherent scenes. In Proceedings of the IEEE IGARSS, Boston, MA, USA, 6–11 July 2008; pp. 457–460.
15. Lombardini, F.; Cai, F. Temporal decorrelation-robust SAR tomography. *IEEE Trans. Geosci. Remote Sens.* **2014**, *52*, 5412–5421. [[CrossRef](#)]
16. Lombardini, F.; Viviani, F. New developments of 4D+ differential SAR tomography to probe complex dynamic scenes. In Proceedings of the IEEE IGARSS, Quebec City, QC, Canada, 13–18 July 2014; pp. 3362–3365.



© 2019 by the authors. Licensee MDPI, Basel, Switzerland. This article is an open access article distributed under the terms and conditions of the Creative Commons Attribution (CC BY) license (<http://creativecommons.org/licenses/by/4.0/>).